Analysis of Flow Characteristics for Different Blade Outlet Angle in LVAD

Devendra Nadaraja[1], Ishkrizat Taib[1,*], Nofrizalidris Darlis[2], Rashidi Kadir[3], Kahar Osman[4], Zahran Khudzari[4]

[1] Faculty of Mechanical Engineering & Manufacturing, University Tun Hussein Onn Malaysia, 86400 Batu Pahat, Johor, Malaysia
[2] Faculty of Technology Engineering, University Tun Hussein Onn Malaysia, 86400 Batu Pahat, Johor, Malaysia
[3] School of Biomedical Engineering and Health Sciences, Faculty of Engineering, Universiti Teknologi Malaysia, 81310 Skudai, Johor, Malaysia
[4] IJN-UTM Cardiovascular Engineering Centre, Institute of Human Centered Engineering, Universiti Teknologi Malaysia, 81310 Skudai, Johor, Malaysia

ARTICLE INFO	ABSTRACT
	Mechanical heart assist device is an emerging treatment for end stage of heart failure which is an alternative to heart transplant due the shortage of heart donors. Despite the clinical success of Left Ventricular Assist Devices (LVAD), the development still continue as new designs are progressively being tested to address the ever existing complications. Developing centrifugal blood pumps requires determination between adequate pump performance while giving attention to possible occurrence of blood clot and damage. This study utilized a proposed design concept of different impeller angle geometry and evaluate its merits of adapting the concept from a perspective of computational fluid dynamic (CFD) approach. Theoretically, two types of impeller angle design feature were chosen for this study, the radial type 90° and backward facing type (50° and 70°) impellers of the blood pump to provide data on both the flow characteristics and pressure distribution of the blood pump (LVAD). Three model variations were constructed from the design parameters for comparison with experimental data. Shear Stress Transport (SST) turbulent model under steady state analysis was used to simulate 3 impeller blade angles with initial boundary setup was known for operating speed and flowrates. Evaluation involved assessing the model variants based on several performance criteria. Ranked selection method was used to rate and select the best performing model variation with a good compromise between the pressure head produced and the percentage of hydraulic efficiency as output level among the geometries. CFD results showed that impeller with blade outlet angle of 50° has the most efficient blood pump configuration among the three types of impeller blades. Pressure gradient drop for this impeller angle is the lowest compared with 90° and 70°. Ranking and selection of the model variants resulted in the backward facing 50° impeller blade ranked as the best performing configuration that gives the good compromise of pump performance setup.

1. Introduction

Ventricular assist device (VAD) is an implantable mechanical device which can partially or fully replace the function of a ventricle of a failing heart [1]. Implantable mechanical blood pumps that

---

assist the circulation of blood by one or both ventricles of the heart have evolved over several decades. Typically blood flows from the left ventricle of the heart into the surgically implanted assist device and pumped out into the aorta via an implanted conduit. The design of the mechanical pump varies (pulsatile fill and pump designs similar to a normal heart and continuous flow rotary pumps). Currently, long-term implantable left ventricular assist devices require an external source of power and control module [2]. Development of blood pumps for adults with end stage heart failure has correspondingly grown at a faster rate than in children. First generation ventricular assist devices (VAD) came into application by adults in 1980s. The use of VAD in children began with the application of adult devices in adolescents [3]. Computational fluid dynamics (CFD) shown impressive progress in the past decade and has evolved into a promising design tool for the development of biomedical devices. It also supports engineers in identifying recirculation areas and other regions with an increased probability for blood clotting [4]. Blade angle is an important factor in determining an excellent flow of blood through LVAD. Impeller geometries through different angle design gives various flow characteristics within flow region of LVAD. Thus, affecting the pressure discharge of the centrifugal blood pump at given rotational speed. Therefore, evaluation of effect of impeller blade angle are the focus of this study. Computational Fluid Dynamics method is used to assess the effect of the impeller design factor on the blood pump efficiency.

The heart is a midline and muscular pump, cone shaped approximately the size of a fist. The inferior surface sits on the central tendon of the diaphragm, and the base faces posteriorly and lies immediately anterior to the oesophagus and descending aorta [5-8]. The cardiac cycle is the process of events that occur when the heart beats. Blood is circulated through pulmonary and systematic circuits during. There are two phases of the cardiac cycle. In the diastole phase, the heart ventricles are relaxed and the heart fills with blood. In the systole phase, the ventricles contract and pump blood out of the heart and to arteries [9-11]. Cardiac system propels blood through the arteries and veins as a function of ventricular contraction. Shortening of cardiac myocytes concentrically results from ventricular motion of heart system due to blood flow [12,13]. Blood hemodynamics in vessels can be represented through few governing equations. Darcy's Law states that blood flow is a function of pressure difference and resistance [14]. Despite numerous medical therapy availability, failure of the cardiac and respiratory systems to provide adequate end organ perfusion and oxygenation often results in the need for mechanical support, either as an adjunct to cardiopulmonary resuscitation or as a bridge to heart transplantation [3,15]. Ventricular assist device (VAD) is an electromechanical device for assisting cardiac circulation, used either to partially or to completely replace the function of a failing heart [16-19]. The first use of mechanical circulatory support in open heart surgery was in 1953, surgical method used a cardiopulmonary bypass machine to repair atrial septal defect in female patient [20]. There are mainly four types of Ventricular assist device (VAD) available regarding the needs of implantation for the heart failure [4,21-23]. Computational Fluid dynamics based design optimization techniques were used to optimize the blade geometries and the flow path to maximize the hydrodynamic performance while minimizing the haemolysis rate [24]. CFD has been used to study the flow fields in blood pumps to estimate pump performance and blood damage potential in the design stages where it is used for comparison and selection of one pump over another [25,26].

2. Methodology

Methodology is a platform to determine the method used for the analysis and the steps needed for data analysis. Computational modelling via CFD is implemented in predicting and evaluating the effect of impeller outlet blade angle of the blood pump on the performance and efficiency. The

performance criteria involved in this study are pressure head and efficiency which are presented as indicators in evaluating the best configuration in term of overall performance.

The research flow chart visualizes the sequential process of methodologies leading to the solution to obtain the best desired modification of blood pump configurations as illustrated in Figure 1. Literature study was done to establish a thorough background on blood pumps used as left ventricular assist device. Various sources were studied to determine the current progress of published works and design concepts where the current study would be based from. Selected design concept was constructed for numerical simulation and validated with comparable publications. Analysis of model configurations involves evaluating performance criteria that was deemed significant on blood pump hemodynamics. Lastly, selection of blood pumps configurations through a ranked selection method to methodically establish the best model variant.
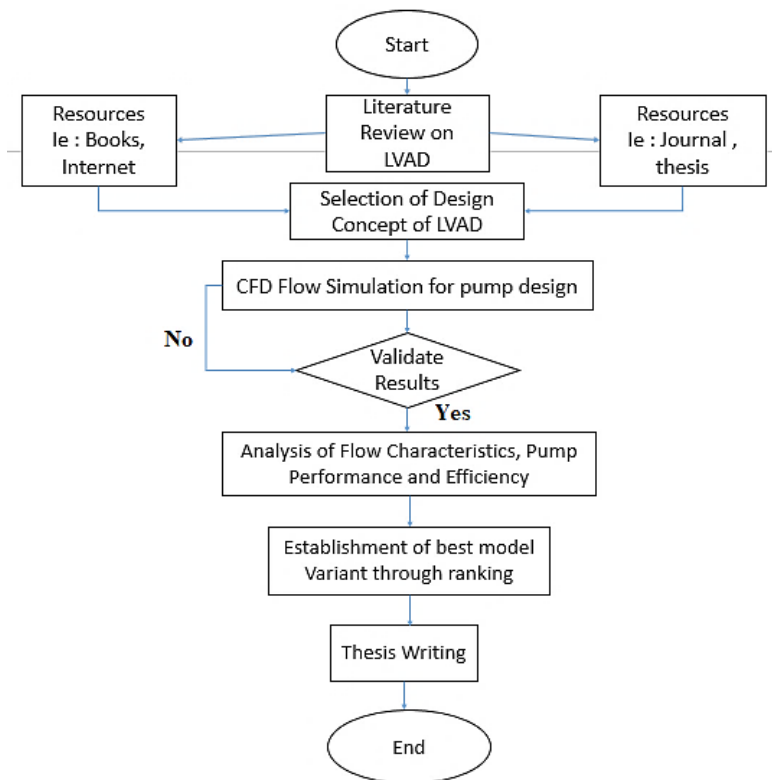

Fig. 1. Methodology Flow Chart

2.1 Governing Equation

In the present study, a comprehensive fluid flow model has been developed using commercial CFD software, FLUENT 19 [4,27]. The salient features of the numerical fluid flow model include temperature and concentration dependent thermo-physical properties such as density, specific heat, thermal conductivity and viscosity. Appropriate model parameters available in FLUENT has been chosen. The effect of normal gravity has also been included in the model. The mass, momentum and species conservation equations are solved along with energy equation. The fundamental equation is employed to describe the flow characteristics in the centrifugal pump, which include two main parts, continuity equation and motion equation, corresponding with mass conservation law and momentum conservation law [28,29].

$$\frac{\partial \rho}{\partial t} + \frac{\partial (\rho u_i)}{\partial x_i} = 0 \tag{1}$$

$$p \frac{\partial u_i}{\partial t} + p u_j \frac{\partial u_i}{\partial x_j} = p - \frac{\partial p}{\partial x_i} + \frac{\partial}{\partial x_j}\left[\left(\frac{\partial u_i}{\partial x_j} + \frac{\partial u_j}{\partial x_i}\right)\right] - \frac{2}{3}\frac{\partial}{\partial x_j}\left(\mu \ \frac{\partial u_j}{\partial x_j}\right) \tag{2}$$

Here, ρ is the density of water. t represents the time. u denotes the velocity. x is the Cartesian coordinate, p is the pressure, μ is the dynamic viscosity.

2.2 Boundary Conditions

Throughout the simulation, a constant angular speed imposed on the impeller rotating fluid region is maintained at three different speed which are 2000 rpm, 3000 rpm, and 4000 rpm. The fluid used in this study is a Newtonian fluid with density and viscosity similar to the characteristic of blood in a human body. Blood can be considered a Newtonian fluid in VAD calculations as the shear rates found in blood pumps is higher than 100 s^{-1}, therefore the viscosity of blood is constant [30,31]. The viscosity of the blood used was 0.035 with the density of 1060 kg/m^3. The inlet pressure of 0 mmHg is used for all models, which is representative of the pressure at the left ventricle during diastole. Three flowrate of the blood pump was chosen within the range of 3-7 L/min, maximum and minimum offset to the design operating speed of 5 L/min to obtain performance characteristics of the pump. The shear stress turbulence (SST) model is selected for this study [4,31]. The SST model was developed to effectively blend the robustness and accuracy of formulation of the k − ω model in the near-wall region with the freestream independence. The SST model is known to perform well in estimating flow separation under adverse pressure gradient [32]. Table 1 shows the studied geometries with boundary conditions applied.

Table 1
Studied impeller geometries with parameters

Impeller Profile	Out Angle Profile (°)	Operating Speed (RPM)	Flow Rate (L/min)
	90	2000 3000 4000	3, 5, 7
	70	2000 3000 4000	3, 5, 7
	50	2000 3000 4000	3, 5, 7

3. Results Analysis and Discussion

In this chapter, the overall performance for the studied blood pump is determined based on performance criteria that will gauge the performance and effectiveness of each configuration of the blood pump variations. The performance variables considered in this analysis are pressure head curve (PQ curve), pump efficiency and prediction of blood damage based on pressure distribution within flow region. Further evaluation of the model configurations was done using a scoring evaluation method typically used for design product evaluation, consisting of screening and scoring method.

3.1 Model Validation

The present computational models are validated against the results reported by Kadir [29] that used 46mm diameter and 5 blade impellers compared to present study that utilized a 44.8mm diameter, 7 blade impeller adapted from the work of Hilton [33]. Comparisons are illustrated in Figure 2. The plot for current study for 2000 rpm is in between the experimental curve of 2000 rpm and 3000 rpm. This comparison was used due to similar impeller size despite the small change in diameter and number of impeller blade, operating speed is one of the known parameters. Unknown parameters generate unyielding proper results between experimental and simulation data. Therefore, graph plots are used for comparison to find similarity in pressure drop within the studied flowrate (3-7 L/min) which are shown in Table 2.
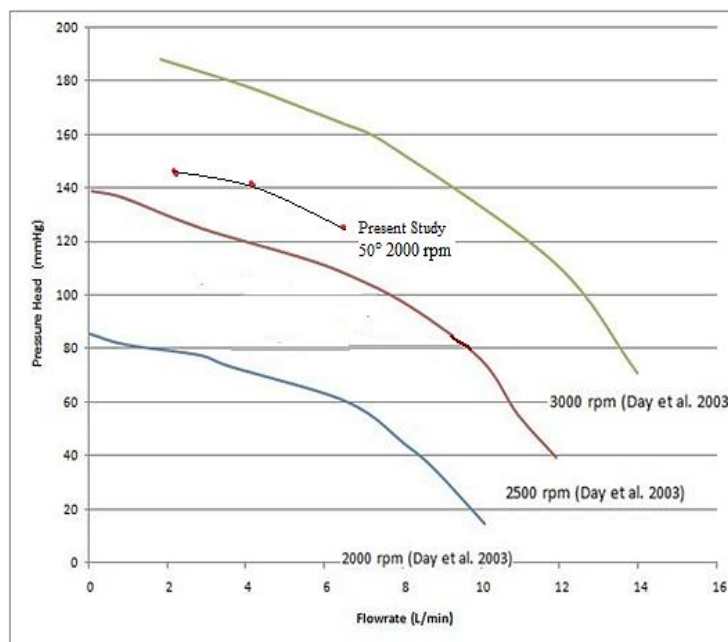

Fig. 2. Comparison of pressure head generated of current study with both numerical and experimental results [34]

Table 2
Pressure head gradient between present study and experimental results [34]

Results	Pressure Head Gradient [mmHg/(L/min)]
3000 rpm - experimental	5.397
2500 rpm - experimental	4.280
Present Study backward facing (50°) 2000 rpm	4.998
2000 rpm - experimental	4.189

3.2 Grid Independence Test

Total of five meshing set up were used to tabulate convergence of the simulation. Pressure head values were observed with different number of elements produced until point of convergence is reached. Table 3 shows the grid independence test data before point convergence is met. Figure 3 illustrates the meshing convergence graph. Skewness is observed as the measure of mesh quality with calculated relative error.

Table 3
Grid Independence Test

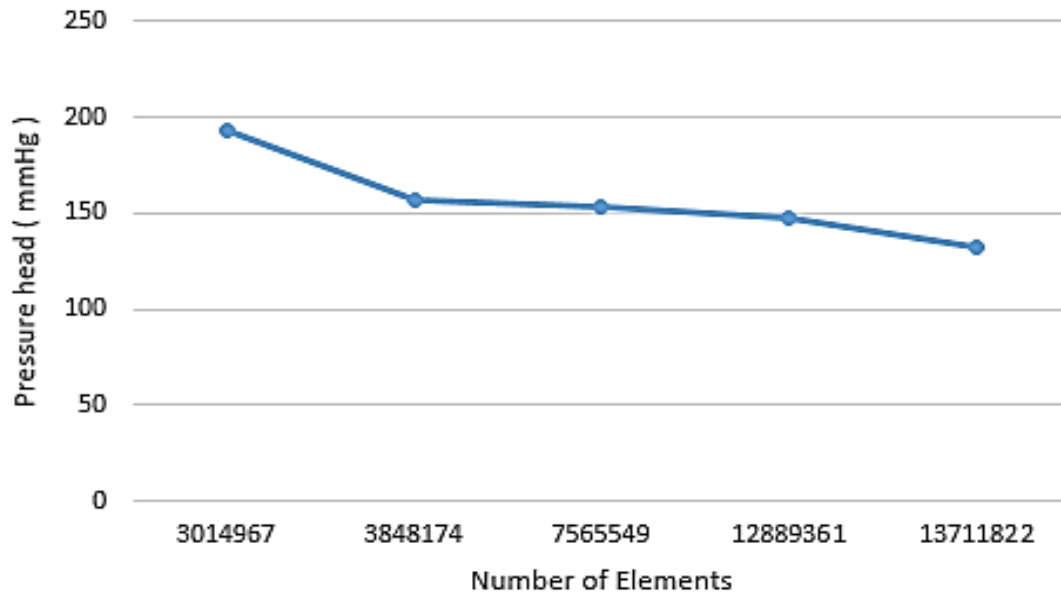| Element Size (mm)	Skewness	Element Number	Pressure Head	Relative Error (%)
0.1	0.8379	13711822	192.43	60.3
0.225	0.7999	12889361	157.12	30.93
0.3	0.7988	7565549	153.42	27.5
0.5	0.7999	3848174	147.99	23.33
0.9	0.8054	3014967	132.57	10.48

Fig. 3. Mesh Convergence graph

3.3 Blood Pump Performance Evaluation
3.3.1 Impeller flow characteristics

Velocity increases from the impeller inlet, then reaching peak value upon exiting the impeller blade. However, velocity begins to drop as the flow continues through volute region, reaching lowest velocity which can be seen at the volute walls as the flow passes the discharge passage. The velocity drop linearly corresponds to pressure rise as the fluid exit the pump. Comparing the velocity contour of both the simulated geometries, radial (90°) impeller blade have a higher velocity profile surrounding the impeller region whereas backward facing (50°) and (70°) impeller blade shows peak velocity near blade faces and tip. Table 4 illustrates the contour plot for three impeller angles geometries for velocity distribution at all operating speed prior to 5 L/min flowrate.

Pressure at the impeller and volute were unevenly distributed across different flowrate. Maximum pressure was located at the volute walls and near the outlet flow region while the pressure is lowest near the back of impeller blades and inlet region. Lower values in pressure in these regions were caused due to high velocity dissipation by the impeller. Table 5 depicts the pressure contour distribution for model geometries, where radial (90°) have slightly higher pressure distribution prior to velocity flow compared to backward (50°) impeller blades at 5L/min flowrate for all operating speed.

Table 4
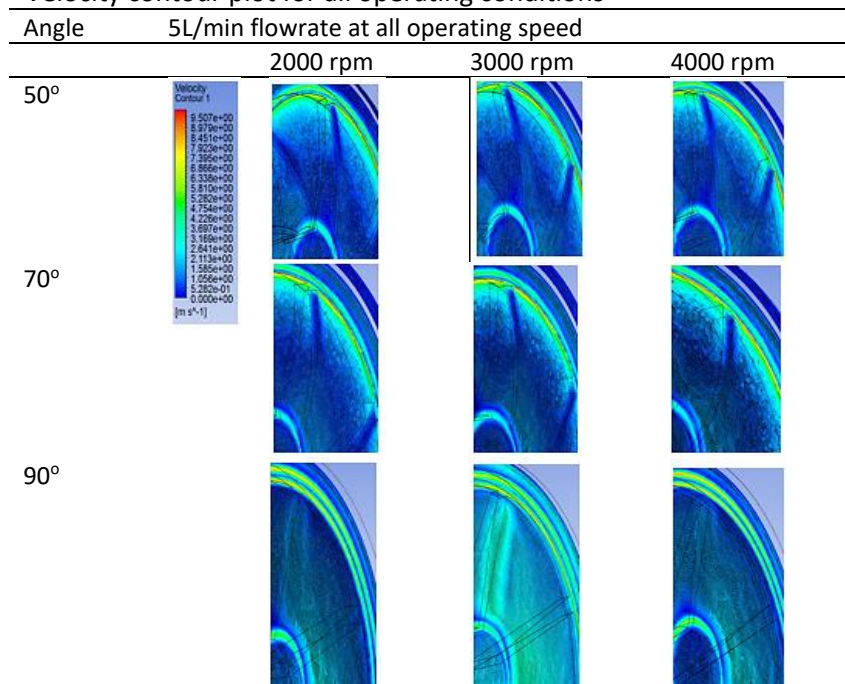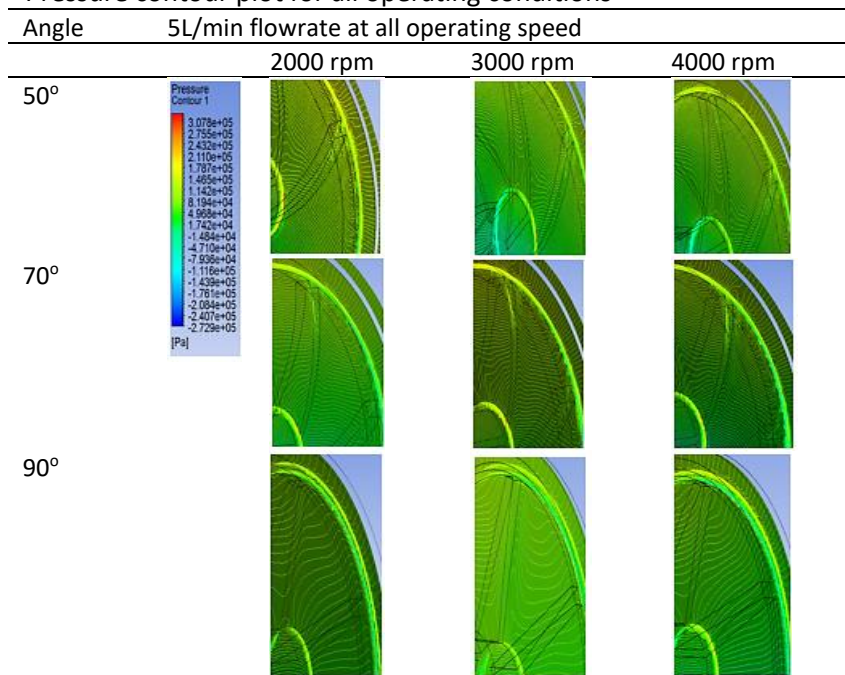Velocity contour plot for all operating conditions

Angle	5L/min flowrate at all operating speed		
	2000 rpm	3000 rpm	4000 rpm
50°			
70°			
90°			

Table 5
Pressure contour plot for all operating conditions

Angle	5L/min flowrate at all operating speed		
	2000 rpm	3000 rpm	4000 rpm
50°			
70°			
90°			

3.3.2 Pressure head performance

Computational data shows that radial (90°) impeller geometry produces 181mmHg, greater than the backward facing (50° and 70°) impeller blades. The model of 50° impeller blades shows drop in generated pressure head. Radial blades show a higher value in pressure head due to the increased angular velocity around the impeller flow region which results in higher pressure distribution inside

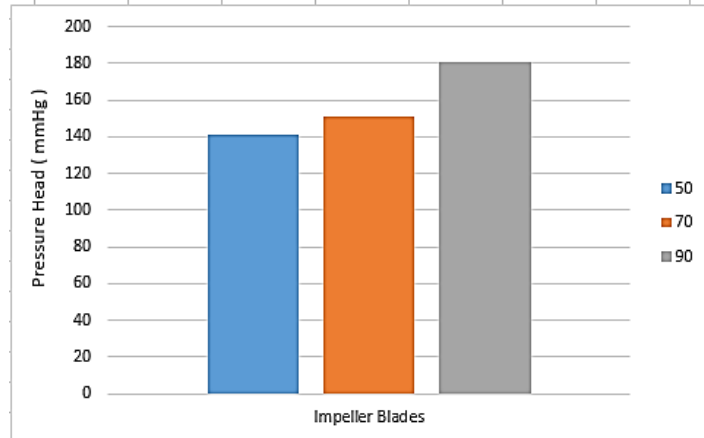the blood pump (LVAD). Figure 4 shows the graphical tabulation between pressure head and impeller blade angle.

Fig. 4. Pressure head at target flowrate at 2000 rpm, 5 L/min for all geometries

Figure 5 illustrates the PQ curve for the varying operating speed, showing the pressure head behavior with increasing flowrate for each model configurations. The general behavior of the pressure head for all the model configurations such that pressure head decreases with increasing flowrate, an expected behavior for centrifugal pumps, was observed throughout all operating speeds. Pressure head value increase with increasing impeller speed, from 2000 to 4000 rpm with increase in magnitude factor. Observation from the figure, showed that all of the model configurations follow a similar pressure head trend.
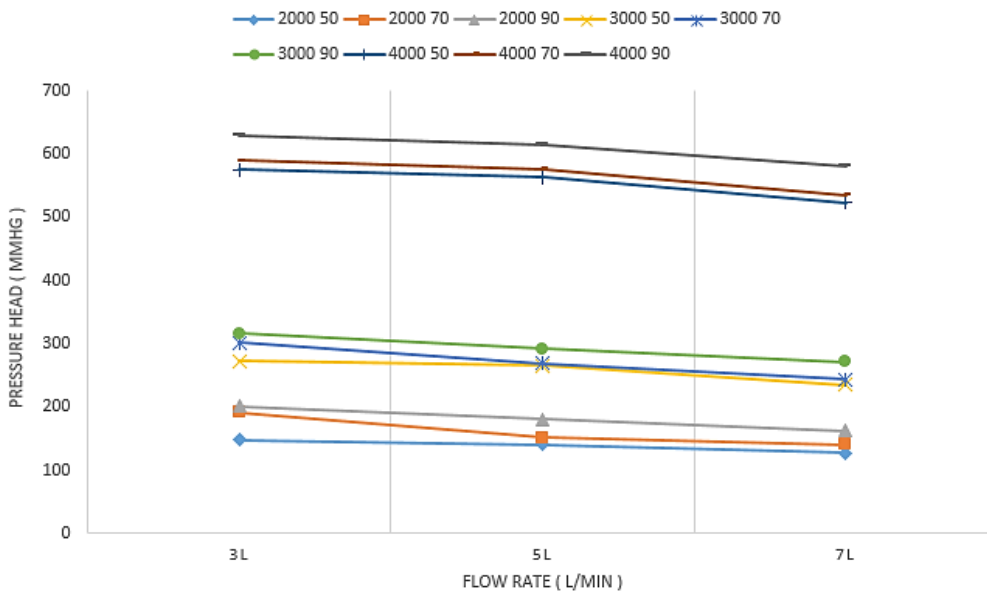

Fig. 5. PQ Curve for all geometry under all boundary condition

The steepness of this curve affects the pressure head of the blood pump. Flatter curve is desirable as pressure head is less sensitive to the changes in flowrate. The overall pressure head gradient for each model geometry is summarized in Figure 6. From the figure it can be observed that radial facing (90°) impeller exhibit a flatter curve with least pressure gradient value compare to backward facing (50°) and (70°) impeller blade.
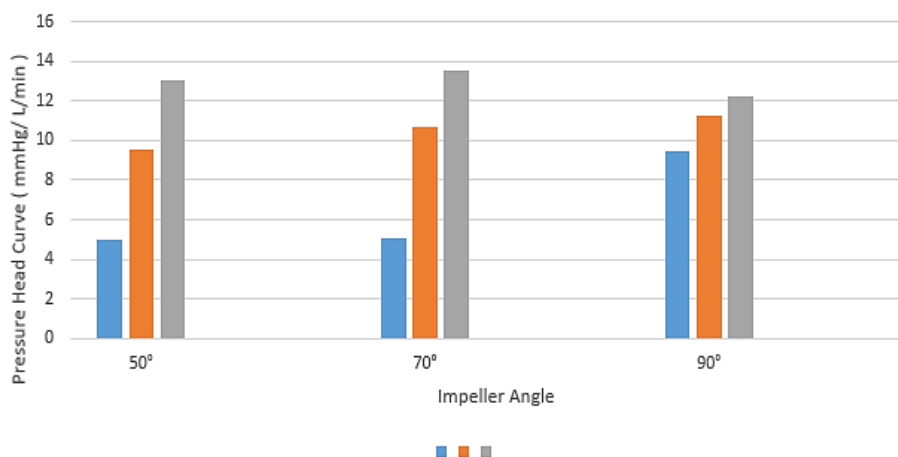
Fig. 6. Pressure head gradient for the model variation

3.3.3 Pump efficiency

Data on torque was gathered before proceeding with efficiency calculations through numerical data. Rotating impeller geometry in this study as mentioned earlier were subjected to torque generation. From the data gathered, increase in rotational speed results in better torque generation. At comparable flowrate, the hydraulic efficiency is observed to drop with each increasing operating speed observed for all geometry configurations. The trend of efficiency increases as the flowrate increases slight and gradually. Figure 7 illustrate the efficiency plot for the studied operating conditions of the blood pump.
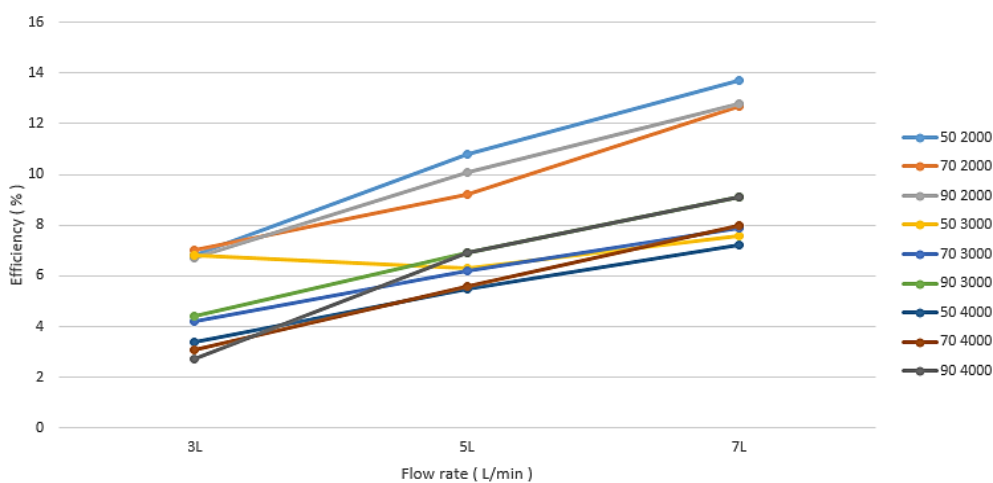
Fig. 7. Pump Efficiency Curve for all impeller geometry

This small increase in trend value indicates that the trend is reaching the best efficiency point (BEP) for each operating speed. The highest peak the trend reaches before dropping in value of efficiency prior to flowrate gradient is considered as the best efficiency point of a pump curve. Therefore, best efficiency point is not observed in this study due to insufficient pressure drop in the efficiency vs flow rate gradient. The efficiency peak for all the operating speed of all the impeller is probably above 7 L /min, beyond the range of study.

3.3.4 Ranked selection of geometry configuration

From the results of various aspects of performance criteria of the blood pump model configurations, a selection method was utilized to evaluate and select the optimum configuration. By using the performance parameters as the design criterion, the model configurations were analysed into scoring stage. The scoring process involves all numerical outputs multiplied to a fraction based on weightage scale where it is determined in Table 6 based on the selected criterion. The superior model configuration would be the model with the smallest net value from all parameters.

Table 6
Weightage value given to result output of model configurations

Parameter	Weightage (%)
Pressure head at design point	40
Pump efficiency at design point	50
Pressure Head Gradient	10

The numerical value of each parameter was multiplied to a predetermined fraction of 100 percent to reflect which parameters were important to the working of a mechanical blood pump. As tabulated in Table 7, efficiency of a blood pump configuration was considered as very important, this is reflected at 50 percent and pressure discharge at the outlet is second important parameter carrying 40 percent weightage. Pressure head gradient carries least amount of weightage 10 percent from the overall weightage.

Table 7
Final score and ranking of geometry

Model Geometry	P_{head}	Rank	Weightage (40%)	Efficiency, η	Rank	Weightage (50%)	$P_{grustlent}$	Rank	Weightage (10%)	Overall Sum	Final Rank
Radial (90°)	181.00	1	7.24	10.1	2	0.505	9.498	3	0.091	7.863	3
Backward (70°)	151.36	2	6.054	9.2	3	0.460	5.077	2	0.051	6.565	2
Backward (50°)	140.99	3	5.640	10.8	1	0.540	4.998	1	0.050	6.230	1

The final value of each model geometry configuration was ranked and final overall score is shown in Table 7. Among these models, radial (90°) impeller type scored the worse with overall marks at 7.836 compared to (70°) impeller blade with a score of 6.565. In comparison among the impeller types, the best overall score was observed with (50°) with a score of 6.230. The value of calculated scoring system is slightly outside the range of experimental data done in previous study. Comparison data between simulated data (present study) does not meet the experimental data range (5.00 – 6.00) in overall score due to some setup problems. However, (50°) impeller angle blade shows have a tolerance of 0.230 which depicts good performance evaluation. Accuracy in scoring criteria can be reduced by further enhancement to the model geometry.

3.4 Discussion

Throughout this study, one selected geometric feature of the blood pump model was studied to evaluate the overall performance and operation of the device. This geometric parameter selected was the impeller outlet blade angle. Three impeller outlet angles were tested via numerical simulation and data tabulated. Rotating element of the centrifugal pump, impeller is a detachable

element inside the blood pump to produce desired fluid discharge rate. Blade outlet angle, defined as the curved region at the tip of the impeller blade, curved in this case depicts the angle value at the exit of the impeller blade.

3.4.1 Effect of impeller angle blade on pressure distribution

From the generated numerical data, pressure increases with the rotational speed of the impeller but decreases across the flowrate gradient. This is due to pressure is inversely proportional to velocity which was illustrated in PQ curve. Higher velocity at impeller flow region leads to pressure drop in impeller region, resulting higher pressure discharge at volute region. Pressure at outlet is related to the velocity discharge at outlet, where pressure raise as velocity drop across a region. Straight radial impeller blades (90°) produce higher velocity flow region as the velocity profile observed at the blade tip, inlet and exit are comparably higher among studied design geometry, where in backward facing impeller blades (50° and 70°) velocity were subjected at relatively smaller region of the impeller blade due to curvature which affects the velocity reading.

3.4.2 Effect of blade angle on efficiency

Efficiency of centrifugal flow blood pump is another studied criterion in this case. In this study, the most efficient pump geometry is the backward facing (50°) impeller. Efficiency shown through the analyses of numerical data depicts that efficiency increases across the three flow rates with decreasing impeller speed. From the plotted data, efficiency curve illustrates that 2000rpm rotational speed produced the highest efficiency prior to its torque generation. Backward facing (50°) produces the highest efficiency leading at 2000 rpm rotational speed subjected to 5L/min flow rate, theoretically minimum requirements needed to operate a blood pump. Data of computational method revealed that curvature of backward facing blades being subjected to velocity profile have lower velocity activity, thus increasing the overall pressure distribution which enhance efficiency of pump with impeller rotational speed and discharge of pressure of the fluid (blood) as output of the pump.

4. Conclusion

This research was conducted to evaluate a design concept for a left ventricular assist device through the use computational fluid dynamic approach. Analysis was carried out to assess the effects of the parameter on the potential pressure distribution and pump performance in terms of efficiency. Selection method was used to further determine the superior configuration with a good compromise between the key performances. Evaluation of the blood pump concept via numerical approach proved beneficial to provide understanding of the effect of each geometric variations of the model on the overall performance thus achieving the objective of this study in evaluating pump flow characteristics and efficiency. The ranking method was applied determining the highest performing model configuration to function as a blood pump. The backward facing (50°) impeller blade scored as the best performing configuration that gives the good compromise of pump performance and discharge of blood, achieved the last objective of the study case.

References

[1] Sawyer, Douglas B., and Ramachandran S. Vasan. *Encyclopedia of Cardiovascular Research and Medicine*. Elsevier, 2017.

[2]   Porepa, Liane F., and Randall C. Starling. "Destination therapy with left ventricular assist devices: for whom and when?." *Canadian Journal of Cardiology* 30, no. 3 (2014): 296-303. https://doi.org/10.1016/j.cjca.2013.12.017

[3]   Adler, Adam C., Kelly L. Grogan, and Laura K. Berenstain. "Mechanical circulatory support." In *A Practice of Anesthesia for Infants and Children*, pp. 500-519. Elsevier, 2019. https://doi.org/10.1016/B978-0-323-42974-0.00021-5

[4]   Marinova, Valeria, Iman Kerroumi, Andreas Lintermann, Jens Henrik Göbbert, Charles Moulinec, Sebastian Rible, Yvan Fournier, and Mehdi Behbahani. "Numerical analysis of the FDA centrifugal blood pump." In *NIC Symposium*, vol. 48, pp. 355-364. 2016.

[5]   Whitaker, Robert H. "Anatomy of the heart." *Medicine* 46, no. 8 (2018): 423-426. https://doi.org/10.1016/j.mpmed.2018.05.010

[6]   Ikwuagwu, Linda. "Anatomy of the Human Heart." *ACLS Training Center*. March 12, 2016. https://www.acls.net/anatomy-of-the-human-heart.

[7]   SEER. "Structure of the Heart." *National Cancer Institute, SEER Training Modules*. Accessed December 2, 2018. https://training.seer.cancer.gov/anatomy/cardiovascular/heart/structure.html.

[8]   Guyton, Arthur C., and John E. Hall. *Text book of medical physiology*. Elsevier, 2006.

[9]   Bailey, Regina. "The Cardiac Cycle." *ThoughtCo*. November 11, 2019. https://www.thoughtco.com/phases-of-the-cardiac-cycle-anatomy-373240.

[10]   Ahmad, Miraj. "Cardiac Cycle, Phases of Cardiac Cycle, Cardiac Cycle & ECG." *Medicosite*. April 10, 2018. https://www.medicosite.com/cardiac-cycle/.

[11]   Lumen Learning. "Cardiac Cycle." *Lumen Learning*. Accessed December 2, 2018. https://courses.lumenlearning.com/suny-ap2/chapter/cardiac-cycle/.

[12]   Pollock, J. D., and A. N. Makaryus. *Physiology, Cardiovascular Hemodynamics*. StatPearls, 2018.

[13]   Secomb, Timothy W. "Hemodynamics." *Comprehensive Physiology* 6, no. 2 (2016): 975. https://doi.org/10.1002/cphy.c150038

[14]   Munson, Bruce R., Donald F. Young, Theodore H. Okiishi, and Wade W. Huebsch. *Fundamentals of fluid mechanics. Sixth ed*. John Wiley & Sons, 2009.

[15]   Carter, B. "Go with the flow." *Innovations in Pharmaceutical Technology* 54 (2015): 36-39.

[16]   Hosseinipour, Milad, Rajesh Gupta, Mark Bonnell, and Mohammad Elahinia. "Rotary mechanical circulatory support systems." *Journal of Rehabilitation and Assistive Technologies Engineering* 4 (2017): 2055668317725994. https://doi.org/10.1177/2055668317725994

[17]   National Heart, Lung, and Blood Institute. "Ventricular Assist Device." *National Heart, Lung, and Blood Institute (NIH)*. Accessed December 3, 2018. https://www.nhlbi.nih.gov/health-topics/ventricular-assist-device.

[18]   Starrh, Laura, and Deborah Becker. "Ventricular assist devices: The basics." *The Journal for Nurse Practitioners* 14, no. 7 (2018): 538-544. https://doi.org/10.1016/j.nurpra.2018.05.001

[19]   Grand View Research. " Congestive Heart Failure Treatment Devices Market Size, Share & Trends Analysis Report By Product (Ventricular Assist Devices, Counter Pulsation Devices, Implantable Cardioverter Defibrillators, Pacemakers) And Segment Forecasts to 2016 – 2024." *Grand View Research*, 2016. https://www.grandviewresearch.com/industry-analysis/congestive-heart-failure-treatment-devices-market

[20]   Lee, P. "Left Ventricular Assist Device (LVAD) and Circulatory Devices in Heart Failure." *Reference Module in Biomedical Sciences* (2018). https://doi.org/10.1016/B978-0-12-801238-3.99664-8

[21]   Pasha Zanous, Sina, Rouzbeh Shafaghat, and Qadir Esmaili. "Numerical investigation of the hydrodynamic parameters of blood flow through stenotic descending aorta." *Proceedings of the Institution of Mechanical Engineers, Part H: Journal of Engineering in Medicine* 229, no. 7 (2015): 524-534. https://doi.org/10.1177/0954411915588574

[22]   Kafagy, Dhyaa, and Horizon Gitano-Briggs. "Axial Flow Artificial Heart Blood Pumps: A Brief Review." *Trends in Biomaterials & Artificial Organs* 27, no. 3 (2013): 124-130.

[23]   Fraser Jr, Charles D., Kathleen E. Carberry, W. Richard Owens, Karol A. Arrington, David LS Morales, Jeffery S. Heinle, and E. Dean McKenzie. "Preliminary experience with the MicroMed DeBakey pediatric ventricular assist device." In *Seminars in Thoracic and Cardiovascular Surgery: Pediatric Cardiac Surgery Annual*, vol. 9, no. 1, pp. 109-114. WB Saunders, 2006. https://doi.org/10.1053/j.pcsu.2006.02.016

[24]   Fan, Hui-min, Fang-wen Hong, Lian-di Zhou, Yin-sheng Chen, Liang Ye, and Zhong-min Liu. "Design of implantable axial-flow blood pump and numerical studies on its performance." *Journal of Hydrodynamics* 21, no. 4 (2009): 445-452. https://doi.org/10.1016/S1001-6058(08)60170-5

[25]   Shi, Yubing, and Theodosios Korakianitis. "Impeller-pump model derived from conservation laws applied to the simulation of the cardiovascular system coupled to heart-assist pumps." *Computers in Biology and Medicine* 93 (2018): 127-138. https://doi.org/10.1016/j.compbiomed.2017.12.012

[26] Bozkurt, Selim, and Koray K. Safak. "Evaluating the hemodynamical response of a cardiovascular system under support of a continuous flow left ventricular assist device via numerical modeling and simulations." *Computational and Mathematical Methods in Medicine* 2013 (2013). https://doi.org/10.1155/2013/986430

[27] Stanfield, J. Ryan, Richard K. Wampler, Jingchun Wu, James Stewart, Trevor A. Snyder, and James W. Long. "Design of a miniature pump for chronic mechanical circulatory support using computational fluid dynamics and flow visualization." In *Frontiers in Biomedical Devices*, vol. 40672, p. V001T01A007. American Society of Mechanical Engineers, 2017. https://doi.org/10.1115/DMD2017-3422

[28] Han, Xiangdong, Yong Kang, Deng Li, and Weiguo Zhao. "Impeller optimized design of the centrifugal pump: A numerical and experimental investigation." *Energies* 11, no. 6 (2018): 1444. https://doi.org/10.3390/en11061444

[29] Kadir, Muhammad Rashidi Abdul. "Numerical Investigation Of Impeller Design Variation On Mechanical Blood Pump Hemodynamics." *PhD diss., Universiti Teknologi Malaysia*, 2017.

[30] Moazami, Nader, Kiyotaka Fukamachi, Mariko Kobayashi, Nicholas G. Smedira, Katherine J. Hoercher, Alex Massiello, Sangjin Lee, David J. Horvath, and Randall C. Starling. "Axial and centrifugal continuous-flow rotary pumps: a translation from pump mechanics to clinical practice." *The Journal of Heart and Lung Transplantation* 32, no. 1 (2013): 1-11. https://doi.org/10.1016/j.healun.2012.10.001

[31] ANSYS. "ANSYS CFX Tutorials 16.0." *ANSYS Inc.*, 2015.

[32] Song, Guoliang, Leok Poh Chua, and Tau Meng Lim. "Numerical study of a centrifugal blood pump with different impeller profiles." *ASAIO Journal* 56, no. 1 (2010): 24-29. https://doi.org/10.1097/MAT.0b013e3181c8f066

[33] Hilton, Andrew. "Proposal for a cost-effective centrifugal rotary blood pump: design of a hybrid magnetic/hydrodynamic bearing." *PhD diss., University of Nottingham*, 2010.

[34] Lin, Changyan, Guanghui Wu, Xiujian Liu, Chuangye Xu, Xiaotong Hou, Haiyang Li, Chen Chen, Peng Yang, Jing Wang, and Yuyang Liu. "In vivo evaluation of an implantable magnetic suspending left ventricular assist device." *The International Journal of Artificial Organs* 38, no. 3 (2015): 138-145. https://doi.org/10.5301/IJAO.2015.14486